



Use of comprehensive screening methods to detect selective human CAR activators

Jenni Küblbeck^{a,*}, Tuomo Laitinen^a, Johanna Jyrkkärinne^a, Timo Rousu^{b,1}, Ari Tolonen^{b,2}, Tobias Abel^a, Tanja Kortelainen^a, Jouko Uusitalo^b, Timo Korjamo^{b,3}, Paavo Honkakoski^a, Ferdinand Molnár^a

^a University of Eastern Finland, Faculty of Health Sciences, School of Pharmacy and Biocenter Kuopio, Yliopistonranta 1C, PO Box 1627, FI-70211 Kuopio, Finland

^b Novamass Ltd, Medipolis Center, Kiviharjuntie 11, FI-90220 Oulu, Finland

ARTICLE INFO

Article history:

Received 21 July 2011

Accepted 31 August 2011

Available online 8 September 2011

Keywords:

Human constitutive androstane receptor

Xenosensors

Agonist

Cell-based assays

Molecular modeling

ABSTRACT

The so-called human xenosensors, constitutive androstane receptor (hCAR), pregnane X receptor (hPXR) and aryl hydrocarbon receptor (hAhR), participate in drug metabolism and transport as well as in several endogenous processes by regulating the expression of their target genes. While the ligand specificities for hPXR and hAhR are relatively well described, this property of hCAR still remains fairly unclear. Identifying hCAR agonists for drug development and for studying hCAR biology are hindered mainly by the unique properties of the receptor, such as the high constitutive activity and complex signaling network but also by the lack of robust and reliable assays and cellular models. Here, validated reporter assays for these three xenosensors are presented and thereafter used to screen a large set of chemicals in order to find novel selective hCAR ligands. We introduce a novel selective hCAR agonist, FL81, which can be used as a stable positive control in hCAR activity assays. Our established receptor-selective ligand identification methods consisting of supporting biological assays and molecular modeling techniques are then used to study FL81 as well as other discovered ligands, such as diethylstilbestrol, *o,p'*-DDT, methoxychlor and permethrin, for their ability to specifically activate hCAR and to regulate the CYP enzyme expression and function.

© 2011 Elsevier Inc. All rights reserved.

1. Introduction

The human constitutive androstane receptor (hCAR, NR113), pregnane X receptor (hPXR, NR12), and the basic helix-loop-helix PER-ARNT-SIM transcription factor aryl hydrocarbon receptor (hAhR) form a trio of ligand-activated transcription factors that regulate drug metabolism and transport [1–3]. Activation of these three receptors, termed as xenosensors, by a diverse set of endogenous and exogenous substances leads to induced expression of their target genes encoding multiple phase I and II metabolic enzymes (e.g. CYP1A2, CYP3A4, CYP2B6, CYP2Cs, UDP-glucuronosyltransferases, sulfotransferases) as well as uptake and efflux transporters (e.g. OATP2, MDR1, MRP2) [4,5]. In addition, glucose and lipid metabolism is modulated by activation of these receptors [6]. Transcriptional processes controlled by these xenosensors depend on their interactions with a large variety of

co-regulator proteins and cross-talk between receptors at the ligand and target gene levels [7,8].

Due to the complexity of regulatory networks and relatively broad ligand specificities of these xenosensors, effects of xenobiotics on CYP and other target gene expression are very difficult to predict in detail. Various in vitro and in silico methods are being used to study the effects of xenobiotics on CYP induction and the transcription factors governing the induction process. Human primary hepatocytes are still the “golden standard” for detecting increases in the CYP activity, protein and mRNA levels despite their limited availability, wide interindividual variability and dedifferentiation in culture [9]. Many factors essential for CYP induction are insufficient in continuous cell lines that remain useful for receptor-specific reporter assays [5]. These reporter assays generally correlate well with induction of specific receptor-regulated CYP isoforms in human primary hepatocytes, as described for AhR and CYP1A [10] and hPXR and CYP3A4 [11]. Different in silico methods can give insights into ligand–receptor and receptor–protein interactions and they have found increasing use in discovery of novel high-affinity, highly specific NR ligands, structure–activity relationships, and rapid classification of compounds [12–14].

The mechanisms of action and ligand specificities of hAhR and hPXR are relatively well described [15–19]. Human AhR agonists

* Corresponding author. Tel.: +358 40 3553875; fax: +358 17 162252.

E-mail address: Jenni.Kublbeck@uef.fi (J. Küblbeck).

¹ Current address: Department of Chemistry, University of Oulu, PO Box 3000, 90014, Oulu, Finland.

² Current address: Admescope Ltd, Kaitoväylä 1F2, 90570 Oulu, Finland.

³ Current address: Orion Corporation, Orionintie 1, PO Box 65, FI-02101 Espoo, Finland.

include dietary flavonoids, endogenous derivatives of tryptophan, bilirubin and lipids, and halogenated polycyclic hydrocarbons [15,20]. The hPXR ligands range from diet-derived flavonoids and vitamin E, endogenous bile acids, therapeutic drugs to environmental contaminants [21,22]. The current list of hCAR activators contains several drugs, environmental chemicals, herbal medicines and flavonoids [21,23–25]. However, only in few cases hCAR agonism has been established with methods other than simple reporter gene assays [26]. The selectivity of these agonists for hCAR over other xenosensors is also often unexplored. This scarcity of information could partly be due to the lack of suitable assays and robust positive reference compounds for hCAR activation. Certainly, a more complex mechanism of hCAR action and significant cross-talk between hCAR and hPXR in the expression of the CYP2B6 gene, also play a role [27,28].

Identifying compounds as hCAR agonists would be important not only for drug development but also for understanding the biological properties of the receptor. The search for novel hCAR agonists is fraught with technical difficulties. First, the high constitutive activity of CAR often interferes with detection of hCAR agonistic ligands in cell-based assays [5,26]. Therefore, inverse agonists for hCAR have been used to lower its basal activity [29,30]. This leads to competition between the added inverse agonist and the tested compounds, and as a result, ligands with weak affinity or partial antagonists might be misclassified. Second, certain hCAR isoforms with splicing variants or artificial mutations display low basal activity [31,32] and they have been proposed as surrogate sensors to detect hCAR ligands. However, these variants affect the structure of the ligand-binding domain (LBD) and presumably might affect the ligand specificity as well. Indeed, differential responses between these variants and the wild-type hCAR have been reported [29,33,34]. Third, cell line-dependent differences may cause wide differences in the extent of hCAR activation and ambiguous assignment of an hCAR ligand. An example of this ambiguity is clotrimazole which has been reported an agonist [35], inverse agonist [36] or inactive [37]. Such contrasting responses may be due to differences in cellular contents of co-activators and co-repressors interacting with nuclear receptors [30,38]. Fourth, the reporter assays for hCAR activation have not been formally validated for screening purposes and calculation of assay performance parameters a posteriori in available reports shows that screening for hCAR activators might have been performed in sub-optimal conditions. The final complicating factor is the so-called indirect activation of hCAR where the compound is able to translocate CAR from the cytosol into the nucleus of a primary hepatocyte but no ligand binding or hCAR trans-activation can be demonstrated *in vitro* [39]. Whether this discrepancy is real or due to above assay-related difficulties is not known.

Our first aim was to formally validate reporter assays for hCAR, hPXR and hAhR to be used in assessment of receptor activation. These validated assays were then used to screen a large chemical library containing novel compounds from virtual screening campaigns and compounds based on literature searches, in order to find novel selective hCAR ligands. We used molecular modeling and supporting biological assays to assess the binding of ligands to hCAR ligand-binding pocket (LBP) and to study the ligand properties required for the specific activation of hCAR, and for CYP induction in human primary hepatocytes.

2. Materials and methods

2.1. Chemicals

Chemicals obtained from virtual screening [30,40] were ordered from Tripos Inc. (St. Louis, MO, USA). All steroids were from Steraloids Inc. (Newport, RI, USA). The synthesis of the

flexible diaryl compounds targeted against estrogen receptor has been described [41]. Tri-*p*-methyl phenyl phosphate (TMPP) and triphenyl phosphate (TPP) were synthesized as described [42]. Phenobarbital (PB) was obtained from Kuopio University Apothecary (Kuopio, Finland). Other chemicals were at least of analytical grade from Sigma–Aldrich Finland (Helsinki, Finland), Riedel de Haën (Seelze, Germany), Calbiochem/Merck Chemicals (Darmstadt, Germany), Synfine Research (Richmond Hill, CA) and Chemos GmbH (Regenstauf, Germany). All chemicals were dissolved and diluted in DMSO, except PB which was dissolved and diluted in H₂O.

2.2. Cell culture

C3A hepatoma cells (ATCC CRL-10741), which express hAhR endogenously, were grown on 100 mm diameter plates in phenol red-free DMEM (Gibco 11880, Invitrogen, Gaithersburg, MD) complemented with 10% FBS (BioWhittaker, Cambrex, Belgium), 1% L-glutamine (Euroclone, Pero (Milano), Italy) and 100 U/ml penicillin–100 µg/ml streptomycin (Euroclone) at 37 °C in 5% CO₂ atmosphere and subcultured once a week. Before transfections, the cells were transferred onto 48-well plates (0.183×10^6 cells/cm²) and cultured overnight. The cells used for transfections were from passages 7 to 25.

2.3. Reporter and cell toxicity assays

C3A cells grown on 48-well plates were transfected for 4 h using the calcium phosphate method with appropriate CMX-GAL4-NR LBD (450 ng/well) or selected hCAR LBD mutants [35], GAL4-responsive UAS4-tk-luciferase (300 ng/well) and pCMVβ (600 ng/well) for the hCAR and hPXR mammalian 1-hybrid (M1H) assays as described [40], or with hAhR-responsive CYP1A1 promoter-driven luciferase (180 ng/well) and pCMVβ (600 ng/well) for the hAhR assay. After transfection, the medium was replaced with fresh DMEM complemented with 5% delipidated serum (HyClone, Logan, UT) and including either the vehicle control (DMSO 0.1%), receptor-activating reference compounds or test chemicals (at 10 µM or selected range). After chemical exposure for 24 h, the cells were lysed and the luciferase and β-galactosidase activities [43] were measured from 20 µl lysate using the Victor² multiplate reader (Perkin Elmer Wallac, Turku, Finland). The luciferase activities were normalized to β-galactosidase activities. Cell toxicity of the compounds was determined with the MTT assay [44].

2.4. Assay validation

The M1H assays were optimized and validated according to NIH guidelines [45] but on 48-well instead of 96-well plates. First, the optimal cell density and plate configuration were determined. Then, dose–response studies with reference compounds were carried out. Finally, two independent 3-plate uniformity assays were conducted, assay performance parameters were calculated and evaluated according to the cut-off values for signal window (SW), Z' factor and assay variability ratio (AVR) listed in Table 2b [46].

2.5. Mammalian 2-hybrid (M2H) assay

The NR interaction domain of human co-activator SRC1 (residues 549–789) was cloned between the NdeI and BamHI sites of the CMX-GAL4-vector. The CMX-GAL4-SRC1 co-regulator construct (250 ng/well) and the VP16-hCAR LBD plasmid (250 ng/well) were co-transfected together with the control plasmid pCMVβ (600 ng) and the luciferase reporter pG5-luc (Promega, Madison, WI) (300 ng/well) into C3A cells and the transfected cells

were treated with selected chemicals or vehicle for 24 h and assayed for reporter activities as described above.

2.6. Induction of CYP mRNA in human primary hepatocytes (HPH)

Primary hepatocytes of a 73-year-old diabetic non-smoker male were obtained from BIOPREDIC International (Rennes, France). The cells were seeded ($0.16\text{--}0.18 \times 10^6/\text{cm}^2$) on collagen I-coated 96-wells in maintenance medium composed of Williams' E medium with Glutamax-1 supplemented with 10% FCS, 100 U/ml penicillin, 100 µg/ml streptomycin, and 4 µg/ml bovine insulin. One day before the start of experiment, the medium was replaced with Williams' E medium supplemented with 2 mM glutamine, 100 U/ml penicillin, 100 µg/ml streptomycin, 4 µg/ml bovine insulin and 50 µM hydrocortisone hemisuccinate (use medium, provided by BIOPREDIC Int.), according to manufacturer's instructions. The cells were exposed for 24 h to reference compounds, test compounds or vehicle DMSO (0.5%, v/v) in triplicate. Cell morphology was observed throughout the study. No clear differences between wells exposed to different chemicals nor any other indications for toxicity were seen. Total RNA was isolated and reverse-transcribed to cDNA by using the TaqMan[®] Gene Expression Cells-to-CT[™] kit components (Applied Biosystems/Ambion Inc., Austin, TX). The cells were washed with ice-cold PBS, lysed with the lysis buffer containing DNase I (50 µl/well) and incubated for 6 min at room temperature. The stop solution (5 µl/well) was added and the plates were incubated for 2 min at room temperature and frozen at -80°C . Complementary DNA was synthesized from 10 µl of each sample according to the manufacturer's instructions.

Real-time quantitative RT-PCR was performed by using TaqMan chemistry on an ABI Prism 7500 instrument and with validated primer/probe sets (Applied Biosystems; Table 1.). The fluorescence data were processed with Eq. (2) in the QGene program [47], and CYP mRNA levels were normalized to the geometric mean of β -actin and GAPDH mRNA expression.

2.7. CYP2B6 and CYP3A4 activity assays

Hepatocytes from the same donor were seeded on 48-well plates and treated as described above, but allowing treatment for 72 h to maximize induction of CYP proteins. After chemical exposure, the chemical medium was replaced with fresh use medium containing 3 mM salicylamide for 30 min to saturate conjugative enzymes. Thereafter, 400 µl of use medium containing 3 mM salicylamide and CYP-specific substrates (1 µM bupropion for CYP2B6 and 1 µM testosterone for CYP3A4) were added to the wells. Samples of 100 µl were withdrawn at 4 h of incubation. The samples were stored at -20°C until analysis of CYP isoform-specific metabolites by LC-MS/MS as described in detail [48].

2.8. CYP inhibition assays

Incubations with cDNA-expressed recombinant CYP3A4 and CYP2B6 enzymes (BD Gentest, Franklin Lakes, NJ) were conducted on 96-well plates essentially as described [49]. The incubation

mixture contained the CYP enzyme (1.4 pmol for CYP3A4 and 0.75 pmol for CYP2B6), probe substrate [50 µM 7-benzyloxy-4-(trifluoromethyl)-coumarin (BFC) for CYP3A4, 2.5 µM 7-ethoxy-4-(trifluoromethyl)-coumarin (HFC) for CYP2B6], 100 mM Tris-HCl buffer, pH 7.4 and NADPH-regenerating system. The test chemicals (FL81 and permethrin) were dissolved in DMSO and added at 0–30 µM final concentrations. Reference inhibitors were ketoconazole (5 µM) and ticlopidine (1 µM) for CYP3A4 and CYP2B6, respectively. After a 10-min preincubation at 37°C , the CYP reactions were initiated by adding 50 µl of NADPH-regenerating system. After 30 min incubation, the reactions were stopped by the addition of the stop solution (80% acetonitrile in 0.1 M Tris). Fluorescence of the 7-hydroxy-4-(trifluoromethyl)coumarin product was measured at 405/535 nm filters with Victor² multiplate reader (Perkin Elmer Wallac, Turku, Finland).

2.9. Recombinant hCAR-LBD protein production

The hCAR LBD (residues 103–348) was cloned into pET-15b expression vector (Novagen) to obtain the N-terminal His₆-hCAR-LBD fusion protein. *Escherichia coli* BL21 (DE3) cells were grown in Luria-Bertani medium and protein production was induced overnight at 20°C with 0.75 mM isopropyl thio- β -D-galactoside. After cell disruption, the fusion protein was purified on a Co²⁺-chelating affinity resin (Clontech), washed and eluted with stepwise additions of imidazole (10, 50, 150, 250 mM) in the purification buffer (50 mM Tris-HCl at pH 8.0, 100 mM NaCl, 10% glycerol). The fractions were assessed using standard SDS-PAGE, and the 50 mM fraction contained high-quality His₆-hCAR-LBD.

2.10. Limited protease digestions (LPD) assay

Under optimized conditions, about 100 pmol of recombinant His₆-hCAR-LBD in the purification buffer was preincubated with DMSO or CAR ligands (final concentration 0.3–10 mM) for 25 min at 25°C in a total volume of 9 µl. Subtilisin A from *Bacillus licheniformis* (Sigma-Aldrich, final concentration 1 ng/µl) was then added, and the digestion was carried out 30 min at 25°C . The reaction was stopped by addition of 3 µl of 5× SDS protein loading buffer (156 mM Tris-HCl at pH 6.8, 5% SDS, 25% glycerol, 0.1% bromophenol blue, 25% saccharose and 1 mM TCEP). The samples were denatured for 5 min at 99°C , resolved by electrophoresis through 16% SDS-PAGE, stained with Coomassie Blue and gel images were captured using ImageQuant System (GE Healthcare Life Sciences).

2.11. Molecular modeling

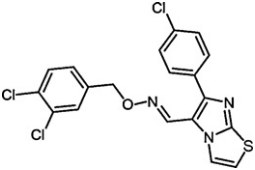
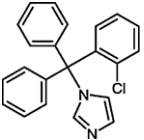
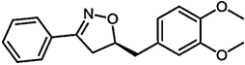
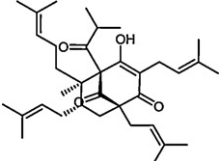
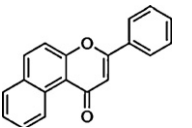
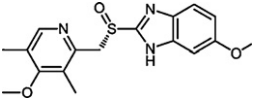
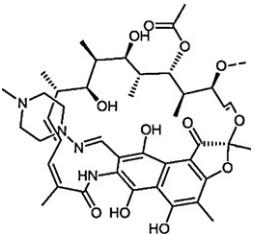
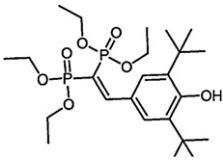
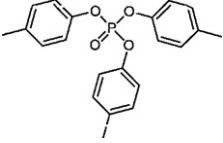
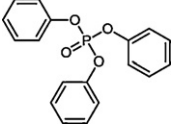
Selected ligands were docked into hCAR LBD (crystal structure 1XVP, chain D) with GOLD docking suite (version 4.0) (Cambridge Crystallographic Database: Cambridge, UK, 2008), and the docking site was defined in GOLD using the ligand molecule (CITCO) extracted from the crystal structure, with a 10 Å distance of the ligand atoms. Side chains of F161 and Y224 were selected as freely moving side chains according to previous MD simulations [50]. The rescoring of the docking poses was performed by calculating binding energies (single point MM-GBSA energies) of ligands using standard MM-GBSA method as implemented in molecular dynamics software AMBER10 [51]. Additionally, contact preference maps of ambiguous docking poses were inspected using the Molecular Operating Environment (MOE) (Chemical Computing Group Inc., Quebec, Canada) and the best pose for each ligand was selected based on both binding energy and adequacy of the interaction fields. For the best poses, MD simulations (1.0 ns) were performed and analyzed with AMBER10.0 package. The trajectories were analyzed for rms-deviations (RMSD), atomic positional

Table 1
Taqman gene expression assays used in the mRNA expression measurements.

Gene	Assay or endogenous control ID	RefSeq
hCYP3A4	Hs00430021_m1	NM_017460.3
hCYP2B6	Hs03044634_m1	NM_000767.4
hCYP1A2	Hs00167927_m1	NM_000761.3
hACTB	4326315E	NM_001101.2
hGAPD	4326317E	NM_002046.3

Table 2a

Selection of positive controls for human CAR, PXR and AhR assays.

	μM	hCAR	hPXR	hAhR
Vehicle (DMSO)	0.1% (v/v)	1.00 ± 0.13	1.00 ± 0.07	1.00 ± 0.04
CITCO	1	$14.59 \pm 1.92^*$	1.92 ± 0.24	$4.35 \pm 0.55^*$
				
Clotrimazole	4	$2.88 \pm 0.05^*$	$11.91 \pm 0.12^*$	$11.94 \pm 0.55^*$
				
FL81	10	$8.29 \pm 0.47^*$	2.79 ± 0.26	1.47 ± 0.16
				
Hyperforin	1	$1.21 \pm 0.10^*$	$26.59 \pm 2.64^*$	1.36 ± 0.07
				
β -Naphthoflavone	10	$7.19 \pm 1.06^*$	0.88 ± 0.13	5.39 ± 1.26
				
Omeprazole (OME)	10	1.02 ± 0.03	$3.18 \pm 0.07^*$	$11.40 \pm 0.27^*$
				
Rifampicin (RIF)	10	1.00 ± 0.04	$12.39 \pm 0.93^*$	1.09 ± 0.06
				
SR12813	5	1.32 ± 0.14	$44.54 \pm 3.14^*$	1.16 ± 0.09
				
TMPP	10	$2.04 \pm 0.25^*$	$4.00 \pm 0.12^*$	$6.34 \pm 0.04^*$
				
TPP	10	$3.66 \pm 0.23^*$	$12.44 \pm 1.27^*$	$6.21 \pm 1.17^*$
				

Data is presented as fold-activation over DMSO vehicle; mean \pm S.E.M. ($n=3$). The ligands chosen as positive controls for the following M1H assays are shown in grey. FL81: 5-(3,4-dimethoxy-benzyl)-3-phenyl-4,5-dihydro-isoxazole; TMPP: tri-p-methyl-phenyl-phosphate; TPP: tri-phenyl-phosphate.

$^* p < 0.05$ vs. vehicle control.

fluctuation (APF) and protein secondary structure with the *ptraj* program of Amber Tools 1.4 [52] and the structures were visually examined with the assistance of the VMD-program [53]. The volume of the LBP was calculated with Voidoo software (Uppsala Software Factory, Uppsala, Sweden). Ligand volumes were calculated by the molecular modeling software Sybyl (Tripos Inc., St. Louis, MO, USA). A more detailed description on the molecular modeling methods is available upon request.

2.12. Data analysis

All biological experiments were performed in triplicates, apart from the inhibition assays (Section 2.8.), which were performed in duplicates. Data are presented as mean \pm S.E.M. The calculation of assay performance parameters is described in Section 2.4. Differences between treatments were compared with the Student's paired *t*-test and considered significant when $p < 0.05$.

3. Results

3.1. Validation of assay protocols for human CAR, PXR and AhR

A small set of hCAR activators along with established hPXR and hAhR ligands was tested in the preliminary experiments in order to find a robust reference compound for large-scale hCAR screening (Table 2a). A novel compound termed FL81 [5-(3,4-dimethoxybenzyl)-3-phenyl-4,5-dihydroisoxazole] from an estrogen receptor-targeted chemical library [41] activated hCAR to much higher degree and was more selective to hCAR than previously used reference compounds TMPP and clotrimazole [40]. The hCAR agonist CITCO [54] had the highest fold-activation in the hCAR M1H assay, but unlike FL81, it gave widely variable responses between assays. We found that the range of fold activation for FL81 was approximately 7- to 13-fold while responses for CITCO varied from 3- to 22-fold in 10 independent experiments, even though both ligands were stored protected from overt light and temperature exposures. Also, the standard deviations between replicates within one experiment were repeatedly larger with CITCO than with FL81. The irreproducible results for CITCO were probably due to its instability, because UV-vis and HPLC-MS determinations indicated structural changes between different CITCO lots (*data not shown*) [29,30]. Therefore FL81 and the established activators rifampicin (RIF) and omeprazole (OME) were chosen as positive controls for hCAR, hPXR and hAhR assays, respectively. Dose-response and uniformity tests were performed according to the NIH guidelines but on 48-well instead of 96-well plates. Based on the results (Table 2b), these reference compounds showed a high specific fold-activation of the cognate receptor, produced reproducible results and lacked any significant toxicity in the MTT assay at the chosen concentrations. The screening assays clearly fulfilled the acceptance criteria for the *Z'*, SW and AVR parameters [46] and remained above thresholds during the screening process. It is significant that no structural modifications of hCAR or additions of inverse agonists were necessary to develop this validated hCAR assay.

3.2. Screening for potential human CAR agonists

Based on our previous virtual screening process described for hCAR ligands [30] and literature searches for human CAR activators and/or CYP2B6 inducers, over 300 compounds were selected and screened for hCAR activation with the validated M1H assay. The final screening concentration was 10 μ M unless literature data suggested higher levels (50–300 μ M) to be used. The cutoff-value for an hCAR agonist was set to a minimum of 4-fold activation over DMSO vehicle control. To control for the specificity of the agonists, hPXR and hAhR assays were performed in parallel. The data for compounds above the hCAR cut-off of 4, were transformed relative to reference-elicited activation for all receptors, listed in Table 3, according to formula (1):

$$E_{\max}(\%) = 100\% \left[\frac{(\text{Act}_{\text{Cmpd}} - \text{Act}_{\text{DMSO}})}{(\text{Act}_{\text{Ref}} - \text{Act}_{\text{DMSO}})} \right] \quad (1)$$

In a similar fashion, E_{\max} values were calculated for those compounds that had previously been reported as hCAR agonists or CYP2B6 inducers but did not reach the cut-off value of 4 in our screening process. Many of the screened hCAR activators proved not to be selective for hCAR but also displayed clear activation of hPXR and/or hAhR. For instance, bergamottin activated all three xenosensors, bupirimate activated both hCAR and hAhR and diethylstilbestrol as well as cypermethrin activated both hCAR and hPXR. Relatively few compounds were hCAR-selective (methoxychlor, *o,p'*-DDT and permethrin) with selectivity ratio above 6 (Table 3.), and their responses were studied further. The estrogenic compound diethylstilbestrol was included to further studies despite its hPXR activity because it has not been shown to activate hCAR in previous studies [55].

3.3. Dose-responses of the selected hCAR agonists

These selected four chemicals along with the reference compounds (FL81 and CITCO) and the so-called indirect activators phenobarbital (PB) and phenytoin (PHN) [56,57] were tested with multiple concentrations with the xenosensor assays (Fig. 1). Strong hCAR activators (response > 8-fold) included CITCO, FL81 and permethrin which activated hCAR maximally at 0.3, 30 or 30 μ M, respectively, without major activation of either hPXR or hAhR. The estrogenic compounds methoxychlor, *o,p'*-DDT and diethylstilbestrol had moderate hCAR activity (4- to 8-fold) and the first two were hCAR-selective up to 3 μ M concentrations. Clotrimazole displayed approximately 3-fold activation at 3 μ M concentration, while the 30 μ M concentration was highly toxic to the cells. As expected, both indirect activators PB and PHN were inactive in the M1H hCAR assay while PB activated hPXR as reported earlier [11]. Apart from CITCO, none of the chemicals showed any activation at low concentrations (<1 μ M). CITCO did not show a dose-dependent increase in hCAR activity but the activity remained close to the maximum with all concentrations.

Table 2b

Performance parameters for the human CAR, PXR and AhR (M1H) assays.

Assay	Chemical	<i>Z'</i>	SW	AVR
hCAR	FL81	0.70	7.82	0.30
hPXR	Rifampicin	0.59	4.65	0.41
hAhR	Omeprazole	0.48	4.25	0.37
Criteria according to Iversen et al. [46]		Excellent: <i>Z'</i> > 0.5	Recommended: SW > 2	Recommended: AVR < 0.6
		Do-able: 0 < <i>Z'</i> > 0.5	Acceptable: SW > 1	Unacceptable: AVR > 0.6
		Yes/no assay: <i>Z'</i> = 0	Unacceptable: SW < 1	
		Unacceptable: <i>Z'</i> < 0		

Table 3The relative extent of receptor activation (E_{\max}) and selectivity for best hCAR activators identified in the screening process.

Compound name	μM	E_{\max} (%)			Selectivity ratio	
		hCAR	hPXR	hAhR	hCAR/hPXR	hCAR/hAhR
Artemisin ^a	100	15.08 \pm 4.60	10.67 \pm 0.56 [*]	24.97 \pm 5.06	1.41	0.60
Bergamottin	10	62.43 \pm 5.94 [*]	45.05 \pm 2.32 [*]	233.70 \pm 16.04 [*]	1.38	0.27
	50	126.70 \pm 0.72 [*]	59.23 \pm 0.10 [*]	188.27 \pm 7.72 [*]	2.14	0.67
Bupirimate	10	60.36 \pm 5.67 [*]	16.07 \pm 0.70 [*]	40.10 \pm 2.64 [*]	3.76	1.50
	50	109.00 \pm 6.20 [*]	20.91 \pm 1.47 [*]	70.60 \pm 8.58 [*]	5.21	1.54
Cerivastatin	50	45.00 \pm 0.77 [*]	79.45 \pm 0.18 [*]	29.86 \pm 2.52 [*]	0.57	1.51
Cypermethrin	10	56.17 \pm 5.36 [*]	44.68 \pm 1.63 [*]	13.13 \pm 0.82 [*]	1.26	4.28
	50	187.33 \pm 19.08 [*]	109.60 \pm 5.96 [*]	29.45 \pm 5.44	1.71	6.36
DEHP ^a	100	23.89 \pm 6.14 [*]	58.75 \pm 3.23 [*]	37.07 \pm 9.61	0.41	0.64
Diethylstilbestrol	10	80.44 \pm 6.00 [*]	21.60 \pm 2.32 [*]	10.49 \pm 0.27 [*]	3.72	7.67
Fenofibrate ^a	200	11.61 \pm 4.60 [*]	18.58 \pm 5.22	10.02 \pm 5.00	0.62	1.16
Fenvalerate	10	52.44 \pm 5.75 [*]	37.65 \pm 2.86 [*]	12.22 \pm 0.37 [*]	1.39	4.29
	50	98.97 \pm 5.17 [*]	91.85 \pm 3.28 [*]	62.57 \pm 4.46 [*]	1.08	1.58
FL29	10	99.03 \pm 5.70 [*]	89.34 \pm 5.97 [*]	14.90 \pm 0.95 [*]	1.11	6.65
FL43	10	31.30 \pm 0.98 [*]	27.10 \pm 1.49 [*]	2.38 \pm 0.20	1.15	13.15
FL44	10	37.39 \pm 1.53 [*]	41.02 \pm 4.47 [*]	7.82 \pm 0.73 [*]	0.91	4.78
FL47	10	46.91 \pm 1.64 [*]	60.51 \pm 8.02 [*]	12.67 \pm 1.24 [*]	0.38	3.70
FL79	10	42.05 \pm 1.65 [*]	121.94 \pm 16.80 [*]	5.11 \pm 0.31	0.34	8.23
FL82	10	100.59 \pm 6.70 [*]	41.89 \pm 2.00 [*]	22.22 \pm 1.78 [*]	2.40	4.52
FL83	10	57.87 \pm 2.97 [*]	58.89 \pm 10.65 [*]	6.20 \pm 0.49	0.98	9.33
Lovastatin	50	151.91 \pm 11.93 [*]	19.76 \pm 1.03 [*]	28.94 \pm 3.85 [*]	7.69	5.25
MBPH ^a	300	12.87 \pm 4.11 [*]	17.60 \pm 0.03 [*]	15.26 \pm 2.95	0.73	0.84
Methoxychlor	10	124.87 \pm 6.37 [*]	18.90 \pm 3.41 [*]	15.05 \pm 1.25 [*]	6.61	8.30
Metolachlor ^a	10	42.29 \pm 5.46 [*]	53.52 \pm 2.00 [*]	5.91 \pm 0.96	0.79	7.15
Mevastatin	50	84.66 \pm 15.42 [*]	13.35 \pm 1.37 [*]	20.06 \pm 3.63	6.34	4.22
<i>o,p'</i> -DDT	10	89.19 \pm 1.54 [*]	14.74 \pm 0.38 [*]	4.09 \pm 0.60	6.05	21.81
Permethrin	10	90.18 \pm 9.09 [*]	14.06 \pm 0.42 [*]	9.73 \pm 0.63 [*]	6.41	9.27
Simvastatin	50	34.07 \pm 5.55 [*]	28.55 \pm 1.13 [*]	22.87 \pm 4.39	1.19	1.49
CITCO	1	148.92 \pm 23.76 [*]	8.62 \pm 0.55	7.56 \pm 0.70	17.28	19.70
FL81	10	100 [*]	26.67 \pm 0.29 [*]	1.71 \pm 0.11	3.75	58.48
Rifampicin	10	25.80 \pm 3.15	100 [*]	3.80 \pm 0.23	0.26	6.79
Omeprazole	10	18.75 \pm 3.05	23.33 \pm 4.60	100 [*]	0.80	0.19

The data is presented as relative fold-activation when positive control is set as 100 (grey); mean \pm S.E.M. ($n=3$). DEHP: di[2-ethylhexyl]-phthalate; FL29: 3-benzyl-5-(2-methoxy-benzyl)-4,5-dihydro-isoxazole; FL43: 5-benzyl-3-(4-methoxy-phenyl)-4,5-dihydro-isoxazole; FL44: 3-hydroxy-1-(4-methoxy-phenyl)-4-phenyl-butan-1-one; FL47: 1-(4-methoxy-phenyl)-4-phenyl-butan-1,3-dione; FL79: 3-hydroxy-1,4-diphenyl-butan-1-one; FL82: 5-benzyl-3-phenyl-4,5-dihydro-isoxazole; FL83: 3,5-diphenethyl-4,5-dihydroisoxazole; MBPH: monobenzyl phthalate.

^a Previously published hCAR activators or CYP2B6 inducers with hCAR activation <4-fold (vs. DMSO set as 1).

^{*} $p < 0.05$ vs. vehicle (DMSO) control.

3.4. Ligand-elicited SRC1 co-activator recruitment

Next, we verified the interactions of these compounds with the hCAR LBD by using an established M2H assay. While the M1H assay measures the net-effect of the recruitment of all cofactors present in the cells, the M2H system assays individual ligand-dependent interactions between the hCAR LBD and the SRC1 co-activator peptide [40,58]. The strong hCAR activators in the M1H assay (CITCO 1 μM , permethrin and FL81 10 μM) displayed a very robust recruitment of the SRC1 peptide by 112-, 94- and 64-fold (Fig. 2). Similarly to the M1H assay, CITCO failed to show a clear dose-dependent increase in hCAR activity. Also, both CITCO and permethrin showed a decrease in reporter activity with high concentrations (30 μM for CITCO and over 10 μM for permethrin). A similar effect was seen with the moderate hCAR activators in the M1H assay (methoxychlor, diethylstilbestrol and *o,p'*-DDT 10 μM), which yielded an activation of 89-, 61- and 43-fold. Clotrimazole showed a 40-fold activation at 10 μM . For clotrimazole, the decrease in activity at higher concentrations is due to its toxicity whereas the other compounds did not show any clear toxicity even at high concentrations. Since the ligands may have different co-activator preferences, EC_{50} values do not necessarily reflect the actual transcriptional response of the receptor [59]. For these reasons, the determination of reliable EC_{50} values for these compounds would be impossible. Finally, the indirect activators PHN and PB which were inactive in the M1H hCAR assay, showed clear dose-dependent enhancement of hCAR LBD interaction with the SRC1 co-activator peptide, up to 12- and 3-fold, respectively.

Also, in this assay, most of the compounds showed an increase in reporter activity also with lower (<1 μM) concentrations (Fig. 2). Thus, the M2H assay is more sensitive in detecting weak hCAR agonists than the M1H assay. Comparison of the M1H and M2H assay results for hCAR showed a good correlation ($r^2 = 0.878$, $n = 9$).

3.5. Protection of the hCAR LBD from proteolysis by agonists

Next, we sought supporting evidence for ligand binding from biochemical experiments with the purified hCAR LBD. It has been shown for several NRs that ligand binding is associated with increased protection from degradation by a variety of proteases in vitro [60–63]. Incubation of the hCAR LBD with subtilisin A resulted in almost complete degradation in the absence of added ligand (Fig. 3, lane 2) while the hCAR ligands appeared to protect hCAR from digestion to various degrees. Often, a triplet of bands appeared on the gel (clotrimazole, CITCO, diethylstilbestrol, *o,p'*-DDT, PB, permethrin) while FL81, methoxychlor and PHN produced at least four bands. FL81 and methoxychlor also displayed strongest protection of the bands with highest molecular weights. Even though we cannot associate any specific protected fragment with the agonistic effect, the data clearly support, for the first time, the direct association in vitro of several ligands with the hCAR LBD. Previously, ligand binding has been demonstrated only for CITCO and 5 β -pregnanedione by co-crystallization and co-activator recruitment with the hCAR LBD [64]. Furthermore, the presence of distinct fragments suggests that the ligands may have different

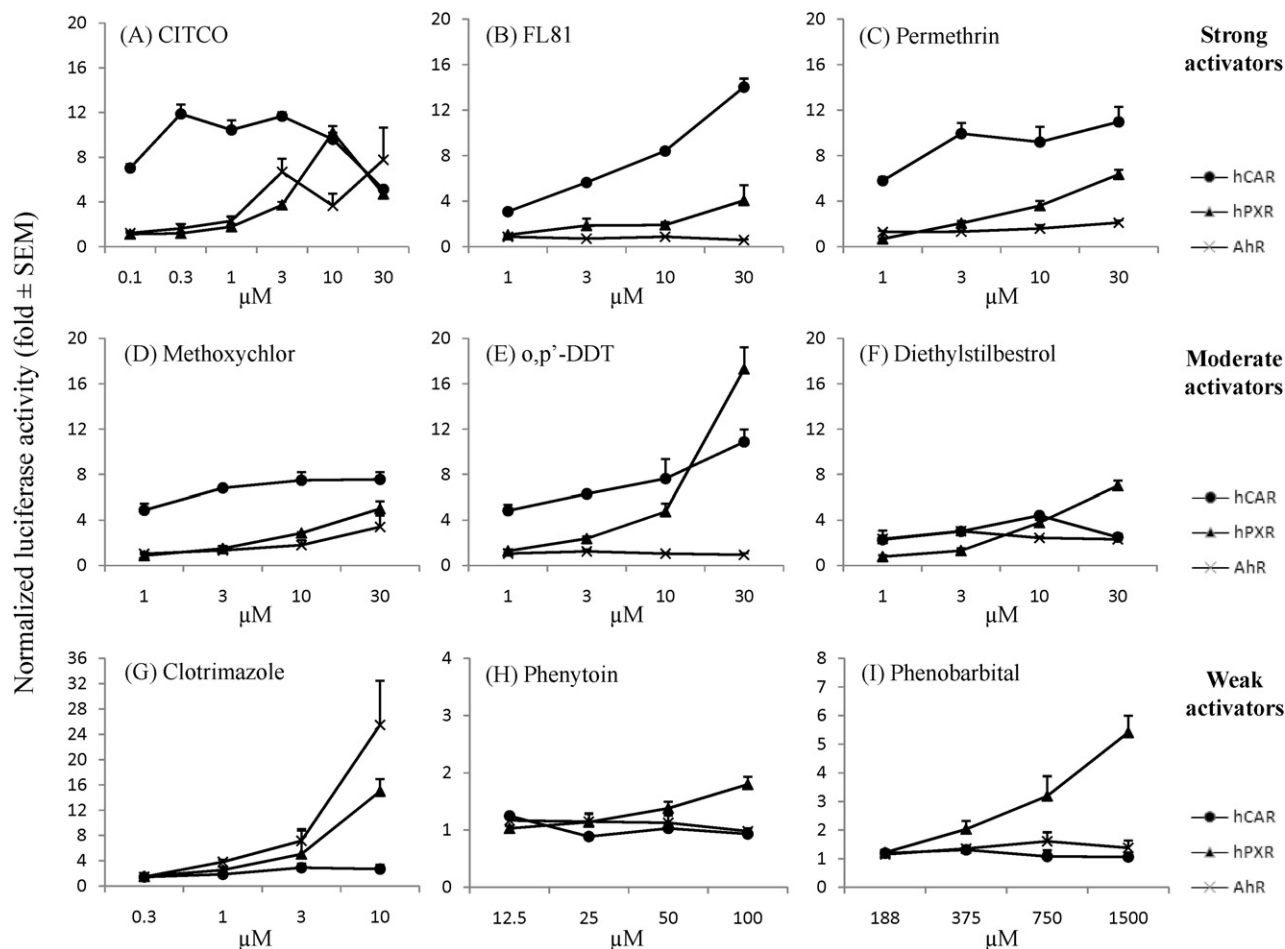


Fig. 1. Dose-responses of hCAR agonists (M1H assay). The ligands are divided into three groups – strong, moderate and weak activators – based on their hCAR activation potential. The results are shown as fold activation (mean \pm S.E.M., $n = 3$). Positive controls ($p < 0.05$ vs. vehicle control): rifampicin 10 μ M, 12.5 ± 0.6 (hPXR); omeprazole 10 μ M, 8.5 ± 1.6 (hAhR) and CITCO 1 μ M, 15.9 ± 1.6 (hCAR). Asterisks indicating statistical significance ($p < 0.05$, test chemical vs. vehicle control) have been omitted for clarity. The statistical significance for receptor activation with these chemicals at 10 μ M concentration has been shown in Tables 2a and 3.

binding orientations within the LBP, presumably due to interactions with specific LBP residues.

3.6. Effects of hCAR LBP mutations on agonist responses

Our previous mutagenesis studies have identified certain crucial LBP residues for hCAR activation [30,35]. Mutagenesis of Y326 to alanine abolished hCAR activation (CITCO, clotrimazole, diethylstilbestrol) or reduced it by 50% or more (TPP, *o,p'*-DDT, methoxychlor, permethrin, FL81). Only clotrimazole was able to activate the F161A mutant (Table 4). This activation might be due to the relatively rigid structure and the central position in the pocket, both of which could compensate the missing residue better than the other ligands (Fig. 6). Mutation of N165 to alanine resulted in both enhanced (CITCO, clotrimazole, TPP, diethylstilbestrol, FL81), reduced (*o,p'*-DDT) or negligible effects (methoxychlor, permethrin) while all agonists could activate the F243A mutant. These divergent data contribute to the idea that specific ligands interact with distinct residues within the hCAR LBP.

3.7. Molecular modeling

There was considerable variation in the efficacies among hCAR agonists in reporter gene activation and recruitment of the SRC1 co-activator peptide. Because the ligand-elicited co-activator recruitment is highly dependent on the position of the NR helix 12 [1,65], we hypothesized that differences in the ligand binding

into the hCAR LBP might elucidate the reasons for dissimilar activation potential by the agonists. Thus, binding of agonists to the hCAR LBP was modeled with dockings and 1.0 ns molecular dynamics (MD) simulations. The analyses of the stability of the helical structure during the MD simulations show that the tested ligands stabilize or destabilize the C-terminal end of hCAR in different ways (Fig. 4). The hCAR C-terminus harbors the activation helix 12 (residues 341–347) which is important for *trans*-activation and co-activator binding. In addition, there is a short helix X (residues 336–339) that is assumed to restrict the movement of helix 12 [64] and thus, thought to keep helix 12 in its active position. However, in the absence of any ligand-free hCAR structure, this notion remains unresolved, and in other NRs, helix X may be associated with ligand binding [66]. Strong agonists such as CITCO and FL81 are able to stabilize both C-terminal helices 12 and X in the active position while permethrin is less efficient in this respect. Clotrimazole, a ligand which has been reported both as an agonist or an inverse agonist, seems to stabilize both helix X and 12 but the position of helix 12 appears to move towards helix 10, out of the assumed optimal position for co-activator binding. Methoxychlor, being one of the weaker activators, is able to stabilize helix 12 but not helix X. The same holds true for PHN which in fact destabilizes helix X and may, consequently, push helix 12 towards helix 10, in a similar fashion with clotrimazole.

In addition, there are differences in the stability of the loop between helices 2 and 3 with different ligands (Fig. 5). The conformation and stability of the loop likely affects the N-terminal

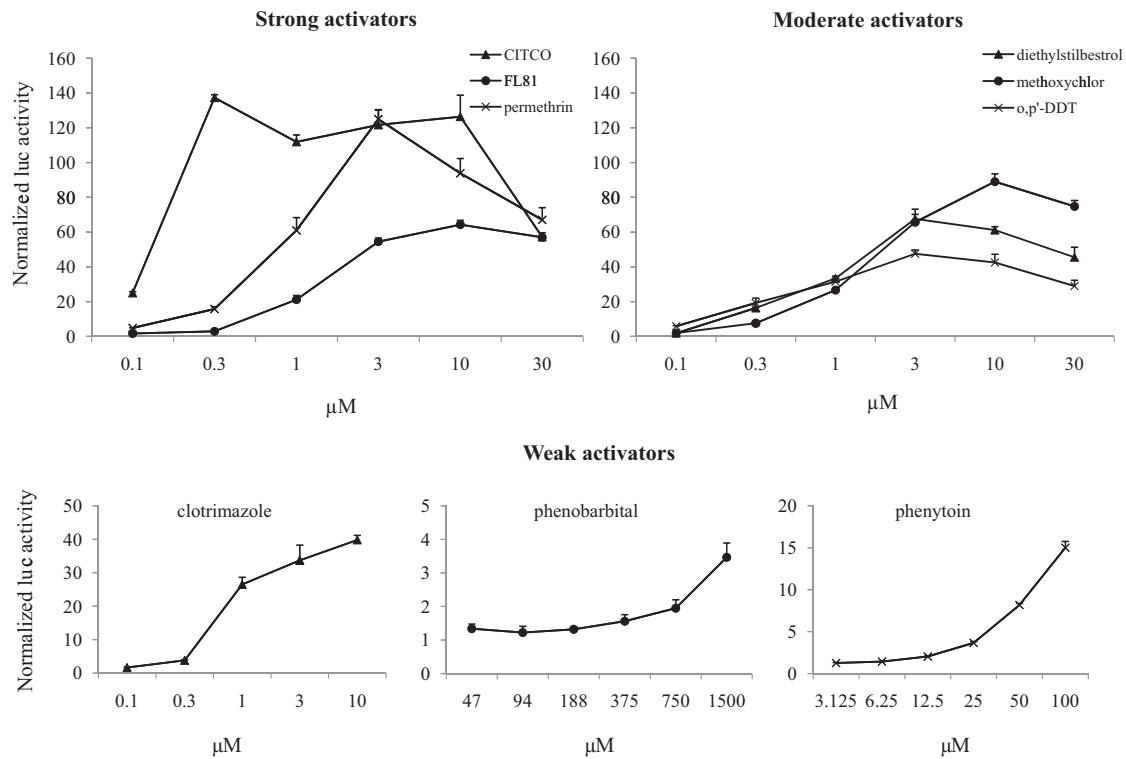


Fig. 2. Ligand-induced SRC1 recruitment (M2H assay), dose-response study. The ligands are divided into the same three groups as in Fig. 1. The results are shown as fold activation (mean \pm S.E.M., $n = 3$). Positive control ($p < 0.05$ vs. vehicle control): CITCO 1 μ M, 152.3 ± 23.3 . Asterisks indicating statistical significance ($p < 0.05$, test chemical vs. vehicle control) have been omitted for clarity.

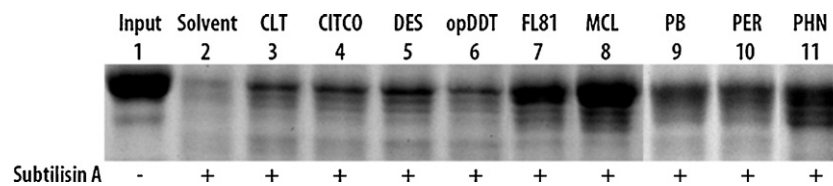


Fig. 3. Limited protease digestion by various human CAR activators. About 100 pmol of purified His₆-hCAR LBD (lane 1, input) was preincubated for 25 min with solvent DMSO (lane 2), or various chemicals [clotrimazole (CLT, lane 3), CITCO (lane 4), diethylstilbestrol (DES, lane 5), *o,p'*-DDT (lane 6), FL81 (lane 7), methoxychlor (MCL, lane 8), phenobarbital (PB, lane 9), permethrin (PER, lane 10) or phenytoin (PHN, lane 11)] at 300 mM each except for PB and PHN at 1 mM final concentration, before a 30-min digestion reaction in the presence of subtilisin A (lanes 2–11).

part of helix 3 which has a resultant effect on neighboring helices X and/or 12. Strong activators such as CITCO seem to stabilize this loop well during the MD run. Permethrin appears to stabilize the loop better than all other ligands, which might contribute to its high activation potential in the reporter assays while FL81 does not stabilize the loop as well as other ligands, which provides a likely

explanation for its weaker ability to promote SRC1 recruitment. In the presence of a moderate activator methoxychlor, the loop is not as stable. Clotrimazole is probably not able to stabilize the loop in an agonist-like manner: only the C-terminal part of the loop is stabilized, which is also the case with a weak activator PHN. Clotrimazole might even destabilize N-terminal part of the loop

Table 4
Reporter assays with hCAR LBP mutations and selected agonists.

Ligand		hCAR				
		wt	Y326A	F161A	N165A	F243A
Vehicle		1.0 \pm 0.2	1.0 \pm 0.1	1.0 \pm 0.3	1.0 \pm 0.1	1.0 \pm 0.2
CITCO	1	12 \pm 3.0*	1.2 \pm 0.4*	1.1 \pm 0.7	20 \pm 15*	30 \pm 9*
Clotrimazole	4	3.1 \pm 0.2*	0.8 \pm 0.03	5.8 \pm 2.8*	22 \pm 0.2*	11 \pm 1.0*
Diethylstilbestrol	10	6.0 \pm 1.1*	0.8 \pm 0.04	1.0 \pm 0.1	9.9 \pm 3.4*	5.7 \pm 0.2*
FL81	10	8.0 \pm 0.002*	2.2 \pm 0.01*	1.1 \pm 0.3	13.4 \pm 1.6*	5.5 \pm 0.1*
Methoxychlor	10	6.6 \pm 0.1*	1.6 \pm 0.1*	1.1 \pm 0.1	5.3 \pm 0.7*	13 \pm 2.4*
<i>o,p'</i> -DDT	10	10 \pm 1.0*	2.8 \pm 0.1*	1.3 \pm 0.03	4.3 \pm 0.6*	19 \pm 1.7*
PB	1500	0.7 \pm 0.1	1.0 \pm 0.2	0.8 \pm 0.1	1.0 \pm 0.1	0.8 \pm 0.1
Permethrin	10	10 \pm 0.4*	5.2 \pm 0.5*	1.1 \pm 0.3	8.0 \pm 1.4*	17 \pm 1.6*
PHN	50	0.7 \pm 0.04	0.7 \pm 0.1	0.7 \pm 0.1	0.9 \pm 0.04	0.9 \pm 0.1
TPP	10	3.5 \pm 0.2*	2.2 \pm 0.3*	1.0 \pm 0.2	18 \pm 1.7*	20 \pm 1.5*

The results are presented as fold (mean) \pm S.E.M. ($n = 3$), vehicle (DMSO) set as 1. None of the chemicals changed the activity of GAL4 only.

* $p < 0.05$ vs. vehicle control.

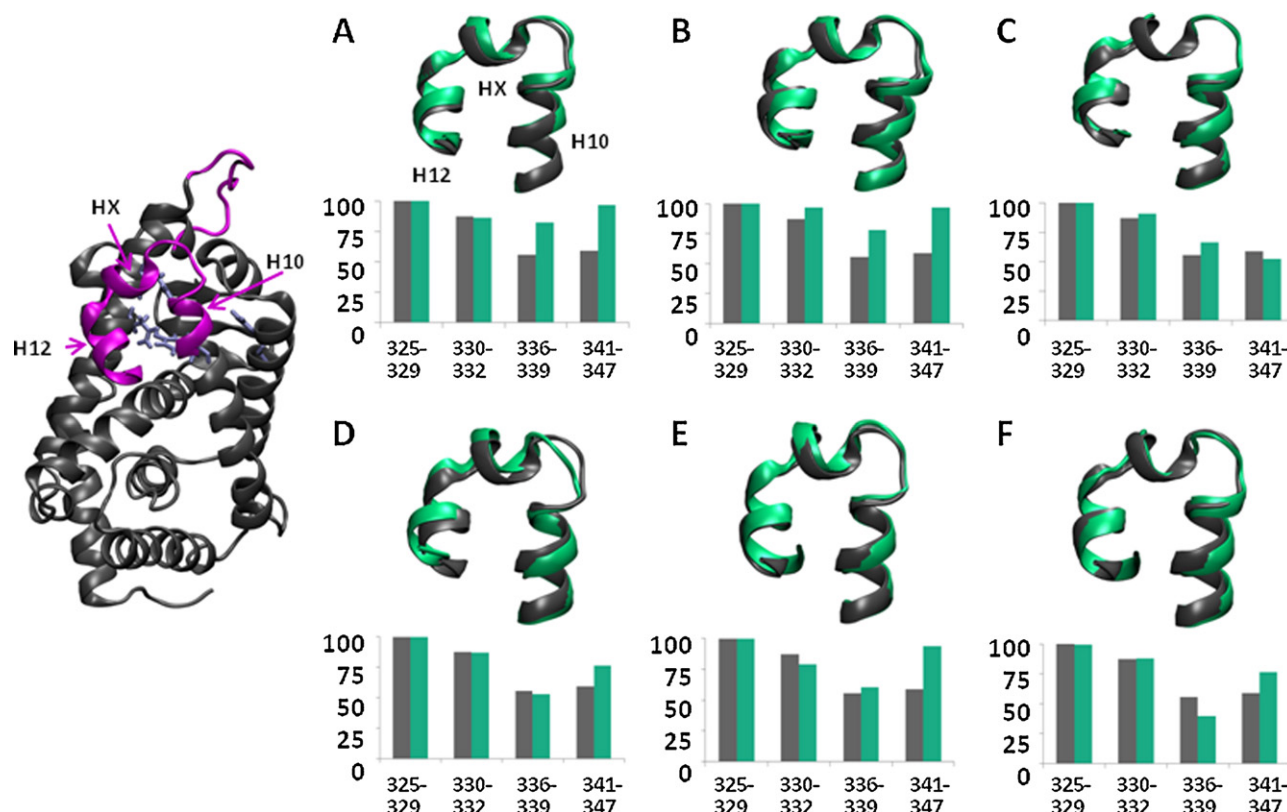


Fig. 4. Conformational changes of C-terminal part of hCAR induced by ligands during the MD simulations. The leftmost figure indicates in *purple* the C-terminal helices 10, X and 12 and the N-terminal loop between helices 2 and 3 within the hCAR LBD, and a selected residues (Y326, F161, N165, F243) lining the pocket are shown in cyan. The top portion in each figures A–F shows the ligand-induced movements of helices 10, X and 12 (represented by *green* ribbons) relative to the *apo* structure (represented by *grey* ribbons). The bottom portions indicate the percentage of time during which residues remain in helical conformation during the MD runs in the presence or absence of ligands (*green* and *grey* bars, respectively). Residues 325–332 are from helix 10, residues 336–339 from helix X and residues 341–347 from helix 12. The selected ligands were CITCO (A), FL81 (B), permethrin (C), methoxychlor (D), clotrimazole (E), and phenytoin (F). (For interpretation of the references to color in this figure legend, the reader is referred to the web version of the article.)

(Fig. 5) (see extension in the pocket with clotrimazole, Fig. 6). These contrasting stabilities at C-terminal helices and at the loop connecting helices 2 and 3 are in line with the dual role reported for clotrimazole in the modulation of hCAR activity. The calculated root mean square deviations (RMSD) of the alpha carbon atoms of CAR show that the structures were stable during the MD runs (see [Supplementary Data, Fig. S1a–j](#)).

We also calculated the relative MM–GBSA interaction energies for the ligands from the 1.0 ns MD simulations and resulting LBP volumes ([Table 5](#)). Generally, there was a good correlation between the activation potential in the M1H and the M2H assays and the interaction energy ($r^2 = 0.876$ and $r^2 = 0.748$, $n = 9$). Also, a relatively good correlation between the size of the ligand as measured by its surface area and the hCAR assays ($r^2 = 0.792$ for M1H and $r^2 = 0.700$ for M2H, $n = 9$). The correlations can be rationalized by placing a large compound such as CITCO within the LBP (Fig. 6): it is able to form many hydrophobic interactions and effectively stabilize the LBD and helix 12 in active position, reflected both in the interaction energy and hCAR activity. Even though only a fraction was occupied by each ligand (26–50%), all agonists appeared to increase the LBP volume significantly (by 17–73%) pointing to the inherent flexibility of the LBP ([Table 5](#)).

3.8. CYP mRNA and activity induction and inhibition

Finally, we tested the ability of the selected agonists to activate expression of hAhR, hCAR and hPXR target genes CYP1A2, CYP2B6 and CYP3A4 in human primary hepatocytes. The FDA-recommended CYP inducers omeprazole (25 μ M), CITCO (0.1 μ M) and

rifampicin (50 μ M) resulted in significant elevation of their target CYP mRNA expression (CYP1A2 246-fold, CYP2B6 16-fold and CYP3A4 9-fold, respectively) indicating that the experimental system was performing well ([Table 6](#)). Apart from *o,p'*-DDT (4- to 8-fold) and methoxychlor (12-fold at 50 μ M), none of the other chemicals showed an increase in CYP1A2 expression (data not shown). PB induced both CYP3A4 and CYP2B6 mRNA by about 3- to 6-fold at 375–750 μ M while PHN was more selective for CYP2B6 over CYP3A4 (about 10-fold vs. 1.5-fold) at 25–100 μ M. This difference can be explained by the facts that PB but not PHN activated also hPXR and that the response of hCAR to PHN in the M2H assay was much stronger than to PB. Diethylstilbestrol activated both CYP isoform mRNAs significantly only at the lowest 3 μ M dose. Of the strong and selective hCAR activators identified in this work, FL81 appeared to induce mRNA expression of CYP2B6 selectively over CYP3A4 (2.5- vs. 0.7-fold at 10 μ M) as compared to *o,p'*-DDT which induced both CYP mRNA isoforms. Intriguingly, methoxychlor was more selective for CYP2B6 than *o,p'*-DDT, as expected from their profile of NR activation ([Fig. 1](#)). The response of FL81 was rather modest and permethrin did not induce the CYP2B6 or CYP3A4 mRNAs to any great extent in 24-h induction period. Nevertheless, we found approximately 2- to 6-fold increases in CYP2B6-mediated bupropion hydroxylase activity by FL81 and permethrin while CYP3A4-mediated testosterone 6 β -hydroxylation was unaffected, which indicates that CYP protein expression was induced by these agonists. These data indicate that the selectivity pattern of CYP2B6 and CYP3A4 induction can be explained mostly by the responses of hCAR and hPXR to these ligands.

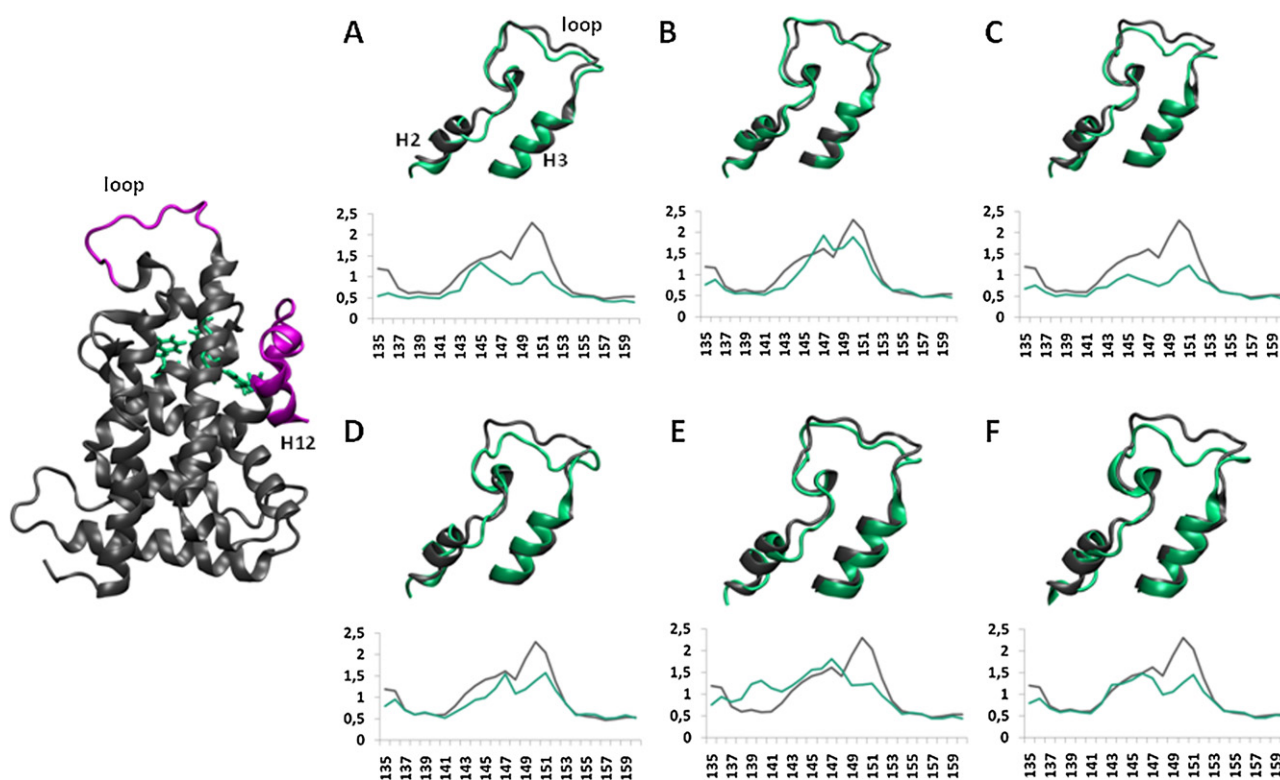


Fig. 5. Stability of the helix 2–helix 3 loop during the MD simulations. The leftmost figure indicates in purple the C-terminal helices 10, X and 12 and the N-terminal loop between helices 2 and 3 within the hCAR LBD, and selected residues (Y326, F161, N165, F243) lining the pocket are shown in green. The top portion in each figures A–F shows the ligand-induced movements of the loop region (represented by green ribbons) relative to the apo structure (represented by grey ribbons). The bottom portions indicate the positional fluctuation of the backbone atoms in residues 135–139 during the MD run. The selected ligands were CITCO (A), FL81 (B), permethrin (C), methoxychlor (D), clotrimazole (E), and phenytoin (F). (For interpretation of the references to color in this figure legend, the reader is referred to the web version of the article.)

The chemical structures and the modest CYP induction responses of permethrin and FL81, while promising in the reporter assays, suggest that these compounds could either inhibit or be metabolized by the enzymes under study. Especially the decrease in CYP2B6 activity with increasing concentrations of FL81 suggested that the compound is a CYP2B6 inhibitor. Therefore, we conducted an inhibition assay with human recombinant CYP2B6 and CYP3A4 (Fig. 7). In this experiment both compounds showed a strong dose-dependent inhibition of CYP3A4 and a more

moderate inhibition of CYP2B6. As far as we know trans-permethrin has previously been shown to be metabolized by esterases both in vitro and in vivo [67]. Preliminary inhibition studies also revealed that several other hCAR activators were also weak (CITCO, MCL) or moderate (*o,p'*-DDT, DES) inhibitors of CYP2B6, and some CYP3A4 inhibition was also observed (*data not shown*). However, whether there is any true relationship between CYP2B6 inhibition and hCAR activation requires a wider array of compounds and remains outside the scope of this study.

Table 5
Properties of hCAR agonists and the hCAR ligand-binding pocket.

	Ligand			Ligand binding pocket (LBP)			Interactions		
	MW (g/mol)	Vol ^a (Å ³)	SA ^b (Å ²)	Vol ^c (Å ³)	%	FD ^d (%)	<Eprot-lig> ^e	hCAR activation (M1H) fold	SRC1 recruitment (M2H) fold
Apo hCAR	–	–	–	476	100	–	–	–	–
Vehicle	–	–	–	–	–	–	–	1	1
Clotrimazole	345	328	299	824	173	40	–34.5	2.9	61
CITCO	437	355	371	748	157	47	–55.0	14.6	175
DES	268	283	273	756	159	37	–19.4	4.4	102
FL81	298	298	304	777	163	38	–40.7	8.3	137
Methoxychlor	346	299	296	704	148	42	–38.5	7.5	181
<i>o,p'</i> -DDT	354	275	217	821	172	34	–36.5	6.8	113
PB	232	215	214	739	155	29	–14.3	1.1	3.5
PHN	252	238	236	555	117	43	–28.4	1.0	5.5
Permethrin	391	375	333	824	173	45	–44.8	9.2	129

^a Ligand volume – Connolly surfaces calculated using Sybyl with set probe radius 1.2 Å.

^b Surface area.

^c LBP volume – Connolly surfaces calculated using Voidoo with the set probe radius 1.2 Å and grid 0.2 Å.

^d Filling degree of the LBP with ligand.

^e Protein–ligand interaction energy.

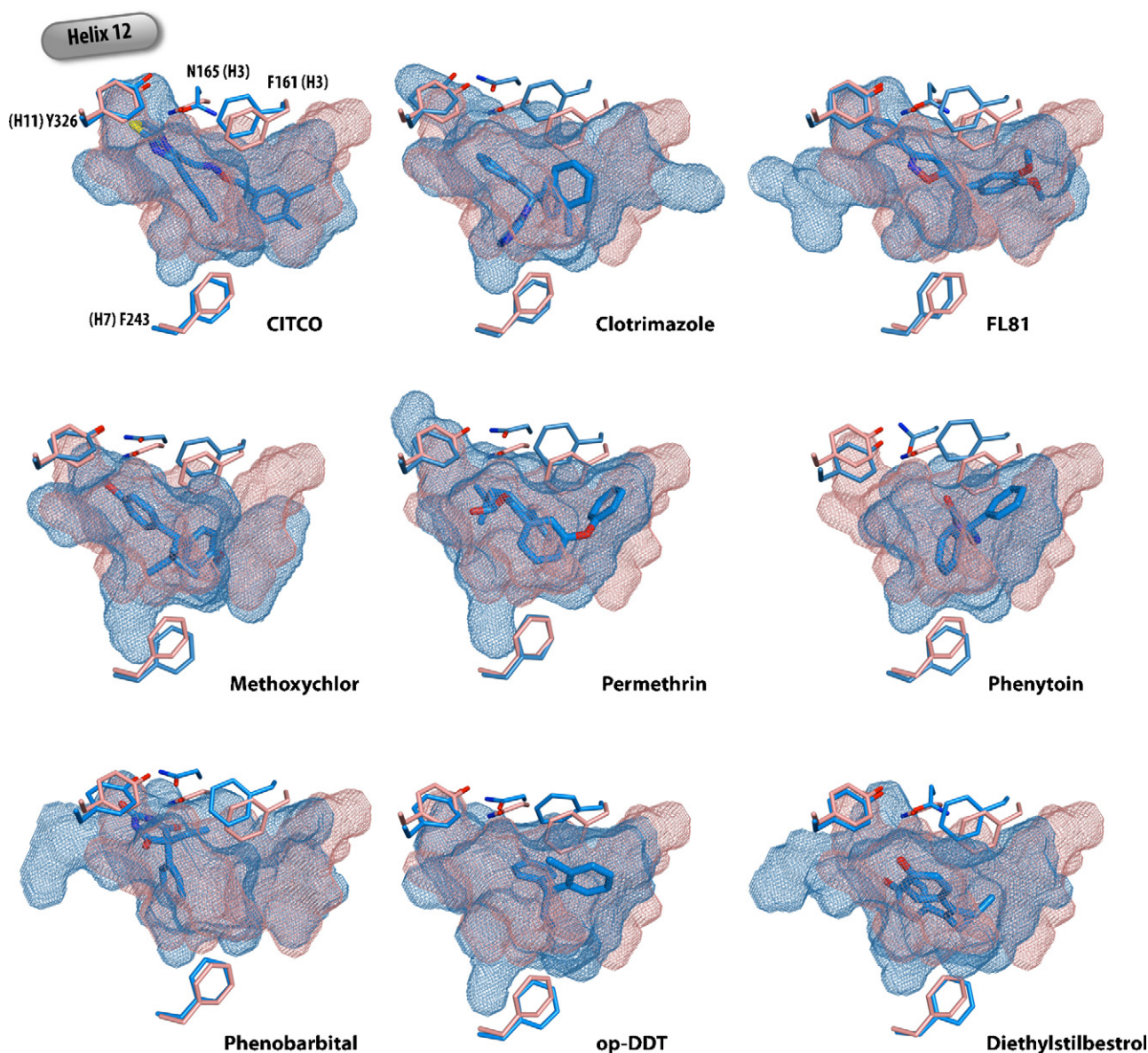


Fig. 6. Modulation of the LBP volume by hCAR ligands. Iso-surface representations of the LBPs of the hCAR-ligand complexes (light blue) compared to superimposed *apo* structure (light brown) were calculated with Voidoo software. Some of the residues (Y326, F161, N165, and F243) crucial for ligand recognition of hCAR are highlighted in the same color code. The position of H12 in the structure is shown in grey oval box. (For interpretation of the references to color in this figure legend, the reader is referred to the web version of the article.)

4. Discussion

Our studies highlight the problems in establishing novel human CAR agonists, which requires very thorough analyses before the identified compounds can be used as reference compounds for *in vitro* assays or as lead compounds for novel hCAR-targeting drug molecules. First, the compounds must be screened with validated assays for activation of hCAR and related receptors. Our previous protocols in HEK293 cells [35,68] have now been improved by the use of human C3A hepatoma cells and carefully optimized transfection conditions. To our knowledge, the current hCAR assay is the first protocol that does not rely on added chemicals or mutated hCAR isoforms to suppress the high hCAR basal activity, thereby avoiding any uncertainties with respect to ligand specificity and/or affinity. Moreover, it is the first validated hCAR protocol with an excellent Z' factor, according to established guidelines and literature [45,46]. Using these validated assays for hAhR, hCAR and hPXR, we have now identified

novel, hCAR-selective activators that are useful as reference compounds in further screening campaigns. The novel compound FL81 and permethrin have the advantage of being cheap and more stable in performance as compared to CITCO. The only drawback of these compounds is their more modest CYP2B6 induction, which probably was due to the metabolism of the compounds or inhibition of CYP enzymes that may hamper their use in human primary hepatocytes.

Such validated assays form a backbone for further structure–activity studies and mechanistic investigations. Our present studies indicate that hCAR agonists are able to increase the volume of the LBP, and they occupy distinct but overlapping regions of the LBP as probed by the molecular modeling and LBP mutagenesis experiments. Thus, it seems plausible that the interactions of the ligands with prominent LBP residues reshape the hCAR binding cavity. These findings indicate that hCAR has a relatively large and flexible LBP, which is in line with the current accumulation of structurally variable ligands for hCAR in the

Table 6
Induction of CYP2B6 and CYP3A4 in human primary hepatocytes.

Ligand	μM	CYP3A4		CYP2B6	
		mRNA expression	CYP activity	mRNA expression	CYP activity
Vehicle		1.00 ± 0.03	1.00 ± 0.09	1.00 ± 0.16	1.00 ± 0.12
CITCO	0.1	1.31 ± 0.04	$1.59 \pm 0.04^*$	$16.34 \pm 1.07^*$	$10.49 \pm 0.31^*$
Rifampicin	50	$9.08 \pm 0.87^*$	$6.76 \pm 0.17^*$	$2.84 \pm 0.38^*$	$12.11 \pm 0.68^*$
FL81	3	0.83 ± 0.18	1.08 ± 0.02	$2.10 \pm 0.35^*$	$2.87 \pm 0.24^*$
	10	0.67 ± 0.17	0.80 ± 0.05	$2.48 \pm 0.14^*$	2.34 ± 0.29
	30	1.45 ± 0.54	0.54 ± 0.07	4.13 ± 0.62	1.38 ± 0.23
Permethrin	3	0.48 ± 0.16	1.07 ± 0.12	0.08 ± 0.002	1.88 ± 0.22
	10	0.30 ± 0.06	1.07 ± 0.03	0.24 ± 0.04	4.48 ± 0.85
	30	0.27 ± 0.03	1.15 ± 0.05	0.51 ± 0.09	$6.04 \pm 0.73^*$
Methoxychlor	10	1.51 ± 0.66	N.D.	4.92 ± 0.23	N.D.
	25	1.47 ± 0.06	N.D.	6.33 ± 1.12	N.D.
	50	$9.96 \pm 0.61^*$	N.D.	$54.28 \pm 5.24^*$	N.D.
<i>o,p'</i> -DDT	3	1.24 ± 0.09	2.18 ± 0.17	1.86 ± 0.34	$8.03 \pm 0.44^*$
	10	2.56 ± 0.53	$2.09 \pm 0.05^*$	$3.44 \pm 0.41^*$	2.05 ± 0.21
	30	2.74 ± 0.73	$2.32 \pm 0.31^*$	4.25 ± 1.16	0.43 ± 0.05
Diethylstilbestrol	3	4.39 ± 0.35	$1.24 \pm 0.04^*$	5.12 ± 2.84	$2.35 \pm 0.13^*$
	10	1.17 ± 0.11	2.00 ± 0.22	1.29 ± 0.43	$3.04 \pm 0.32^*$
	30	0.66 ± 0.09	$1.64 \pm 0.09^*$	0.47 ± 0.14	$2.29 \pm 0.10^*$
Phenytoin	25	1.30 ± 0.63	1.30 ± 0.17	$9.99 \pm 3.54^*$	6.05 ± 1.58
	50	1.65 ± 0.65	$1.46 \pm 0.06^*$	12.01 ± 1.96	$6.71 \pm 0.13^*$
	100	0.69 ± 0.25	$1.81 \pm 0.18^*$	12.43 ± 2.53	$7.44 \pm 1.40^*$
Phenobarbital	375	$2.85 \pm 0.41^*$	1.62 ± 0.22	6.75 ± 0.53	$4.21 \pm 0.79^*$
	750	5.48 ± 2.46	$2.37 \pm 0.10^*$	5.89 ± 0.25	5.55 ± 1.26
	1500	5.54 ± 2.24	$1.92 \pm 0.04^*$	27.69 ± 6.62	$6.82 \pm 0.54^*$

Data is presented as fold-activation over DMSO vehicle; mean \pm S.E.M. ($n=3$).

* $p < 0.05$ vs. vehicle control.

literature. We also provide evidence that increasing the surface area of the ligand and providing specific interactions with the LBP correlates with enhanced co-activator recruitment and activation of the target gene. It should be borne in mind though that there are limits to the LBP flexibility because we have shown that ligand occupancy near helix 12 can lead to decreased agonistic activity [30]. Together with our present and previous modeling studies, the binding by hCAR is governed by mostly hydrophobic interactions which lead to general stabilization of the LBD, as demonstrated by limited protease experiments.

Our evidence indicates that the M2H assay to test for hCAR activation seems to be a promising addition to the M1H

measurements. The M2H assay is more sensitive and hence, it is able to find also weak agonists. The extent of activation recorded in the M2H assays is on average 11-fold stronger than in regular M1H assays for the tested compounds, while the correlation between these two assays was rather excellent ($r^2 = 0.876$). The minor discrepancies between the results could be explained by the fact that only one co-activator is included in a single M2H assay whereas several cellular co-activators are present and able to interact with the hCAR LBD in the M1H assay. Although no activation by PHN and PB took place in the M1H assay, the more sensitive M2H assay provided evidence that PHN, and to lesser extent also PB, can bind directly to the hCAR LBD. Supporting results from limited protease digestion indicated that PHN and PB can protect hCAR LBD from degradation, and the degree of protection correlated with the extent of activation in the M2H assay. These findings suggest that, at least for some ligands that seemingly do not activate hCAR, the role of the so-called indirect activation should be re-examined in view of potentially sub-optimal conditions for receptor activation assays. The latest findings on PB-elicited indirect activation is that the residue T38 in mouse CAR is dephosphorylated in response to PB and activated CAR is then translocated into nucleus [69]. However, the residue corresponding to T38 is not present in hCAR LBD constructs in either of our assays. This suggests that even weak ligands can interact with the hCAR LBD, and the T38 dephosphorylation-translocation process might be a consequence of the ligand recognition by the hCAR LBP. Such a scenario might eliminate the need for two distinct mechanisms for hCAR activation.

Acknowledgements

We thank Lea Pirskanen and Julia Groß for their valuable help with the reporter assays and protease digestions, respectively. This study was supported by the Academy of Finland (F.M., P.H.).

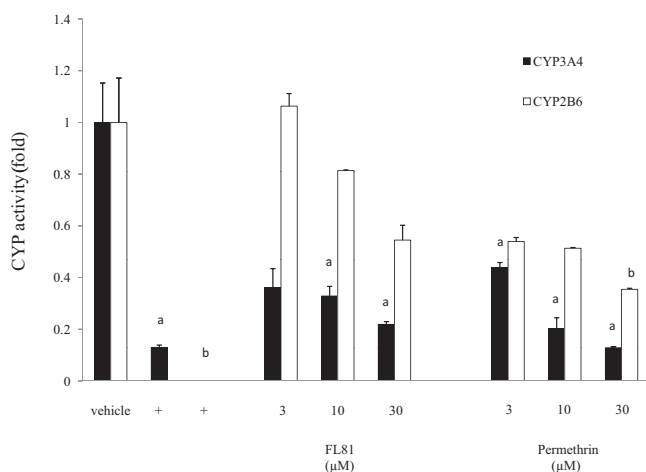


Fig. 7. CYP3A4 and CYP2B6 enzyme inhibition by selected hCAR activators. Results are shown as fold-activity (mean \pm S.E.M., $n=2$) over vehicle control (DMSO) set as 1. Positive inhibitor controls: ketoconazole 5 μM (CYP3A4) and ticlopidine 1 μM (CYP2B6). ^a $p < 0.05$ vs. vehicle (CYP3A4), ^b $p < 0.05$ vs. vehicle (CYP2B6).

Appendix A. Supplementary data

Supplementary data associated with this article can be found, in the online version, at doi:10.1016/j.bcp.2011.08.027.

References

- [1] Bain DL, Heneghan AF, Connaghan-Jones KD, Miura MT. Nuclear receptor structure: implications for function. *Annu Rev Physiol* 2007;69:201–20.
- [2] Grönemeyer H, Gustafsson JA, Laudet V. Principles for modulation of the nuclear receptor superfamily. *Nat Rev Drug Discov* 2004;3:950–64.
- [3] Köhle C, Bock KW. Coordinate regulation of human drug-metabolizing enzymes, and conjugate transporters by the Ah receptor, pregnane X receptor and constitutive androstane receptor. *Biochem Pharmacol* 2009;77:689–99.
- [4] Ma Q. Induction of CYP1A1. The AhR/DRE paradigm: transcription receptor regulation, and expanding biological roles. *Curr Drug Metab* 2001;2:149–64.
- [5] Pelkonen O, Turpeinen M, Hakola J, Honkakoski P, Hukkanen J, Raunio H. Inhibition and induction of human cytochrome P450 enzymes: current status. *Arch Toxicol* 2008;82:667–715.
- [6] Gao J, Xie W. Pregnane X receptor and constitutive androstane receptor at the crossroads of drug metabolism and energy metabolism. *Drug Metab Dispos* 2010;38:2091–5.
- [7] Pascucci JM, Gerbal-Chaloin S, Drocourt L, Maurel P, Vilarem MJ. The expression of CYP2B6, CYP2C9 and CYP3A4: a tangle of networks of nuclear and steroid receptors. *Biochim Biophys Acta* 2003;1619:243–53.
- [8] Tompkins LM, Wallace AD. Mechanisms of cytochrome P450 induction. *J Biochem Mol Toxicol* 2007;21:176–81.
- [9] Hewitt NJ, Lechón MJ, Houston JB, Hallifax D, Brown HS, Maurel P, et al. Primary hepatocytes: current understanding of the regulation of metabolic enzymes and transporter proteins, and pharmaceutical practice for the use of hepatocytes in metabolism, enzyme induction, transporter, clearance and hepatotoxicity studies. *Drug Metab Rev* 2007;39:159–234.
- [10] Sugihara K, Okayama T, Kitamura S, Yamashita K, Yasuda M, Miyairi S, et al. Comparative study of aryl hydrocarbon receptor ligand activities of six chemicals in vitro and in vivo. *Arch Toxicol* 2008;82:5–11.
- [11] Luo G, Cunningham M, Kim S, Burn T, Lin J, Sinz M, et al. CYP3A4 induction by drugs: correlation between a pregnane X receptor reporter gene assay and CYP3A4 expression in human hepatocytes. *Drug Metab Dispos* 2002;30:795–804.
- [12] Ai N, Krasowski MD, Welsh WJ, Ekins S. Understanding nuclear receptors using computational methods. *Drug Discov Today* 2009;14:486–94.
- [13] Bisson WH, Koch DC, O'Donnell EF, Khalil SM, Kerkvliet NI, Tanguay RL, et al. Modeling of the aryl hydrocarbon receptor (AhR) ligand binding domain and its utility in virtual ligand screening to predict new AhR ligands. *J Med Chem* 2009;52:5635–41.
- [14] Ekins S, Kortagere S, Iyer M, Reschly EJ, Lill MA, Redinbo MR, et al. Challenges predicting ligand-receptor interactions of promiscuous proteins: the nuclear receptor PXR. *PLoS Comput Biol* 2009;5:e1000594.
- [15] Denison MS, Nagy SR. Activation of the aryl hydrocarbon receptor by structurally diverse exogenous and endogenous chemicals. *Annu Rev Pharmacol Toxicol* 2003;43:309–34.
- [16] Carnahan VE, Redinbo MR. Structure and function of the human nuclear xenobiotic receptor PXR. *Curr Drug Metab* 2005;6:357–67.
- [17] Kawajiri K, Fujii-Kuriyama Y. Cytochrome P450 gene regulation and physiological functions mediated by the aryl hydrocarbon receptor. *Arch Biochem Biophys* 2007;464:207–12.
- [18] Kliewer SA, Goodwin B, Willson TM. The nuclear pregnane X receptor: a key regulator of xenobiotic metabolism. *Endocr Rev* 2002;23:687–702.
- [19] Ohtake F, Fujii-Kuriyama Y, Kato S. AhR acts as an E3 ubiquitin ligase to modulate steroid receptor functions. *Biochem Pharmacol* 2009;77:474–84.
- [20] Ashida H, Nishiumi S, Fukuda I. An update on the dietary ligands of the AhR. *Expert Opin Drug Metab Toxicol* 2008;4:1429–47.
- [21] Stanley LA, Horsburgh BC, Ross J, Scheer N, Wolf CR. PXR and CAR: nuclear receptors which play a pivotal role in drug disposition and chemical toxicity. *Drug Metab Rev* 2006;38:515–97.
- [22] Sinz M, Kim S, Zhu Z, Chen T, Anthony M, Dickinson K, et al. Evaluation of 170 xenobiotics as transactivators of human pregnane X receptor (hPXR) and correlation to known CYP3A4 drug interactions. *Curr Drug Metab* 2006;7:375–88.
- [23] Hernandez JP, Mota LC, Baldwin WS. Activation of CAR and PXR by dietary, environmental and occupational chemicals alters drug metabolism, intermediary metabolism and cell proliferation. *Curr Pharmacogenomics Person Med* 2009;7:81–105.
- [24] Kretschmer XC, Baldwin WS. CAR and PXR: xenosensors or endocrine disruptors? *Chem Biol Interact* 2005;155:111–28.
- [25] Chang TK, Waxman DJ. Synthetic drugs and natural products as modulators of constitutive androstane receptor (CAR) and pregnane X receptor (PXR). *Drug Metab Rev* 2006;38:51–73.
- [26] Poso A, Honkakoski P. Ligand recognition by drug-activated nuclear receptors PXR and CAR: structural, site-directed mutagenesis and molecular modeling studies. *Mini Rev Med Chem* 2006;6:937–47.
- [27] Wang H, Negishi M. Transcriptional regulation of cytochrome P450 2B genes by nuclear receptors. *Curr Drug Metab* 2003;4:515–25.
- [28] Maglich JM, Stoltz CM, Goodwin B, Hawkins-Brown D, Moore JT, Kliewer SA. Nuclear pregnane x receptor and constitutive androstane receptor regulate overlapping but distinct sets of genes involved in xenobiotic detoxification. *Mol Pharmacol* 2002;62:638–46.
- [29] Dring AM, Anderson LE, Qamar S, Stoner MA. Rational quantitative structure-activity relationship (RQSAR) screen for PXR and CAR isoform-specific nuclear receptor ligands. *Chem Biol Interact* 2010;188:512–25.
- [30] Jyrkkärinne J, Windshügel B, Rönkkö T, Tervo AJ, Küblbeck J, Lahtela-Kakkonen M, et al. Insights into ligand-elicited activation of human constitutive androstane receptor based on novel agonists and three-dimensional quantitative structure-activity relationship. *J Med Chem* 2008;51:7181–92.
- [31] DeKeyser JG, Stagliano MC, Auerbach SS, Prabhu KS, Jones AD, Omiecinski CJ. Di(2-ethylhexyl) phthalate is a highly potent agonist for the human constitutive androstane receptor splice variant CAR2. *Mol Pharmacol* 2009;75:1005–13.
- [32] Chen T, Tompkins LM, Li L, Li H, Kim G, Zheng Y, et al. A single amino acid controls the functional switch of human constitutive androstane receptor (CAR) 1 to the xenobiotic-sensitive splicing variant CAR3. *J Pharmacol Exp Ther* 2010;332:106–15.
- [33] DeKeyser JG, Laurenzana EM, Peterson EC, Chen T, Omiecinski CJ. Selective phthalate activation of naturally occurring human constitutive androstane receptor splice variants and the pregnane X receptor. *Toxicol Sci* 2011;120:381–91.
- [34] Auerbach SS, Stoner MA, Su S, Omiecinski CJ. Retinoid X receptor- α -dependent transactivation by a naturally occurring structural variant of human constitutive androstane receptor (NR1I3). *Mol Pharmacol* 2005;68:1239–53.
- [35] Jyrkkärinne J, Windshügel B, Mäkinen J, Ylisirniö M, Peräkylä M, Poso A, et al. Amino acids important for ligand specificity of the human constitutive androstane receptor. *J Biol Chem* 2005;280:5960–71.
- [36] Moore LB, Parks DJ, Jones SA, Bledsoe RK, Consler TG, Stimmel JB, et al. Orphan nuclear receptors constitutive androstane receptor and pregnane X receptor share xenobiotic and steroid ligands. *J Biol Chem* 2000;275:15122–7.
- [37] Toell A, Kröncke KD, Kleinert H, Carlberg C. Orphan nuclear receptor binding site in the human inducible nitric oxide synthase promoter mediates responsiveness to steroid and xenobiotic ligands. *J Cell Biochem* 2002;85:72–82.
- [38] Liu Z, Auboeuf D, Wong J, Chen JD, Tsai SY, Tsai MJ, et al. Coactivator/corepressor ratios modulate PR-mediated transcription by the selective receptor modulator RU486. *Proc Natl Acad Sci USA* 2002;99:7940–4.
- [39] Swales K, Negishi M. CAR, driving into the future. *Mol Endocrinol* 2004;18:1589–98.
- [40] Küblbeck J, Jyrkkärinne J, Poso A, Turpeinen M, Sippl W, Honkakoski P, et al. Discovery of substituted sulfonamides and thiazolidin-4-one derivatives as agonists of human constitutive androstane receptor. *Biochem Pharmacol* 2008;76:1288–97.
- [41] Pulkkinen JT, Honkakoski P, Peräkylä M, Berczi I, Laatikainen R. Synthesis and evaluation of estrogen agonism of diaryl 4,5-dihydroisoxazoles, 3-hydroxyketones, 3-methoxyketones and 1,3-diketones: a compound set forming a 4D molecular library. *J Med Chem* 2008;51:3562–71.
- [42] Honkakoski P, Palvimo JJ, Penttilä L, Vepsäläinen J, Auriola S. Effects of triaryl phosphates on mouse and human nuclear receptors. *Biochem Pharmacol* 2004;67:97–106.
- [43] Honkakoski P, Jääskeläinen I, Kortelahti M, Urtti A. A novel drug-regulated gene expression system based on the nuclear receptor constitutive androstane receptor (CAR). *Pharm Res* 2001;18:146–50.
- [44] Mosmann T. Rapid colorimetric assay for cellular growth and survival: application to proliferation and cytotoxicity assays. *J Immunol Methods* 1983;65:55–63.
- [45] Assay Guidance Manual Version 5.0, 2008. Eli Lilly and Company and NIH Chemical Genomics Center. Available online at: http://www.ncgc.nih.gov/guidance/manual_toc.html [last accessed Jan 12, 2011].
- [46] Iversen PW, Eastwood BJ, Sittampalam GS, Cox KL. A comparison of assay performance measures in screening assays: signal window, Z' factor, and assay variability ratio. *J Biomol Screen* 2006;11:247–52.
- [47] Müller PY, Janovjak H, Miserez AR, Dobbie Z. Processing of gene expression data generated by quantitative real-time RT-PCR. *Biotechniques* 2002;32:1372–4. 1376, 1378–9.
- [48] Tolonen A, Petsalo A, Turpeinen M, Uusitalo J, Pelkonen O. In vitro interaction cocktail assay for nine major cytochrome P450 enzymes with 13 probe reactions and a single LC/MS–MS run: analytical validation and testing with monoclonal anti-CYP antibodies. *J Mass Spectrom* 2007;42:960–6.
- [49] Salminen KA, Meyer A, Jerabkova L, Korhonen LE, Rahnasto M, Juvonen RO, et al. Inhibition of human drug metabolizing cytochrome P450 enzymes by plant isoquinoline alkaloids. *Phytomedicine* 2011;18:533–8.
- [50] Windshügel B, Jyrkkärinne J, Poso A, Honkakoski P, Sippl W. Molecular dynamics simulations of the human CAR ligand-binding domain: deciphering the molecular basis for constitutive activity. *J Mol Model* 2005;11:69–79.
- [51] Case DA, Darden TA, Cheatham III TE, Simmerling CL, Wang J, Duke RE, et al. AMBER 10. San Francisco: University of California; 2008.
- [52] Case DA, Cheatham 3rd TE, Darden T, Gohlke H, Luo R, Merz Jr KM, et al. The Amber biomolecular simulation programs. *J Comput Chem* 2005;26:1668–88.
- [53] Humphrey W, Dalke A, Schulten K. VMD: visual molecular dynamics. *J Mol Graph* 1996;14:33–8.
- [54] Maglich JM, Parks DJ, Moore LB, Collins JL, Goodwin B, Billin AN, et al. Identification of a novel human constitutive androstane receptor (CAR) agonist and its use in the identification of CAR target genes. *J Biol Chem* 2003;278:17277–83.

- [55] Kawamoto T, Kakizaki S, Yoshinari K, Negishi M. Estrogen activation of the nuclear orphan receptor CAR (constitutive active receptor) in induction of the mouse Cyp2b10 gene. *Mol Endocrinol* 2000;14:1897–905.
- [56] Kawamoto T, Sueyoshi T, Zelko I, Moore R, Washburn K, Negishi M. Phenobarbital-responsive nuclear translocation of the receptor CAR in induction of the CYP2B6 gene. *Mol Cell Biol* 1999;19:6318–22.
- [57] Wang H, Faucette S, Moore R, Sueyoshi T, Negishi M, LeCluyse E. Human constitutive androstane receptor mediates induction of CYP2B6 gene expression by phenytoin. *J Biol Chem* 2004;279:29295–301.
- [58] Repo S, Jyrkkärinne J, Pulkkinen JT, Laatikainen R, Honkakoski P, Johnson MS. Ligand specificity of constitutive androstane receptor as probed by induced-fit docking and mutagenesis. *J Med Chem* 2008;51:7119–31.
- [59] Nettles KW, Greene GL. Ligand control of coregulator recruitment to nuclear receptors. *Annu Rev Physiol* 2005;67:309–33.
- [60] Leid M. Ligand-induced alteration of the protease sensitivity of retinoid X receptor alpha. *J Biol Chem* 1994;269(19):14175–81.
- [61] Nayeri S, Carlberg C. Functional conformations of the nuclear 1alpha,25-dihydroxyvitamin D3 receptor. *Biochem J* 1997;327(Pt 2):561–8.
- [62] Camp HS, Li O, Wise SC, Hong YH, Frankowski CL, Shen X, et al. Differential activation of peroxisome proliferator-activated receptor-gamma by troglitazone and rosiglitazone. *Diabetes* 2000;49:539–47.
- [63] García-Becerra R, Cooney AJ, Borja-Cacho E, Lemus AE, Pérez-Palacios G, Larrea F. Comparative evaluation of androgen and progesterone receptor transcription selectivity indices of 19-nortestosterone-derived progestins. *J Steroid Biochem Mol Biol* 2004;91:21–7.
- [64] Xu RX, Lambert MH, Wisely BB, Warren EN, Weinert EE, Waitt GM, et al. A structural basis for constitutive activity in the human CAR/RXRalpha heterodimer. *Mol Cell* 2004;16:919–28.
- [65] Jin L, Li Y. Structural and functional insights into nuclear receptor signaling. *Adv Drug Deliv Rev* 2010;62:1218–26.
- [66] Windshügel B, Jyrkkärinne J, Vanamo J, Poso A, Honkakoski P, Sippl W. Comparison of homology models and X-ray structures of the nuclear receptor CAR: assessing the structural basis of constitutive activity. *J Mol Graph Model* 2007;25:644–57.
- [67] Takaku T, Mikata K, Matsui M, Nishioka K, Isobe N, Kaneko H. In vitro metabolism of trans-permethrin and its major metabolites, PBalc and PBacid, in humans. *J Agric Food Chem* 2011;59:5001–5.
- [68] Jyrkkärinne J, Mäkinen J, Gynther J, Savolainen H, Poso A, Honkakoski P. Molecular determinants of steroid inhibition for the mouse constitutive androstane receptor. *J Med Chem* 2003;46:4687–95.
- [69] Mutoh S, Osabe M, Inoue K, Moore R, Pedersen L, Perera L, et al. Dephosphorylation of threonine 38 is required for nuclear translocation and activation of human xenobiotic receptor CAR (NR113). *J Biol Chem* 2009;284:34785–92.